

Seminar @ School of Physics and Astronomy  
Queen Mary University of London



**Sensitivity of accelerator based short baseline  
neutrino experiments to  $\nu$ -electron scattering  
radiative corrections**

Célio A. Moura – UFABC  
with Omar Miranda and Guadalupe Moreno – CINVESTAV  
18 November 2021



$$\nu e \rightarrow \nu e$$

## radiative correction study motivation

- Intense neutrino beams improve the statistics for analysis;
- Possibility to test with high precision the standard model predictions;
- Clean measurement of precise electroweak predictions;
  - Possible contribution from Neutrino Charge Radius.

For details: <https://doi.org/10.1103/PhysRevD.104.013007>

# Tree level cross section

The differential cross section for the  $\nu_\mu e^-$  scattering at tree level is given by

$$\frac{d\sigma}{dT} = \frac{2m_e G_F^2}{\pi} \left\{ g_L^2 + g_R^2 \left( 1 - \frac{T}{E_\nu} \right)^2 - g_R g_L m_e \frac{T}{E_\nu^2} \right\}, \quad (1)$$

where  $m_e$  is the electron mass,  $G_F$  is the Fermi constant,  $T$  is the electron kinetic energy of recoil, and  $E_\nu$  is the incoming neutrino energy. The coupling constants  $g_L$  and  $g_R$  are defined at tree level, as

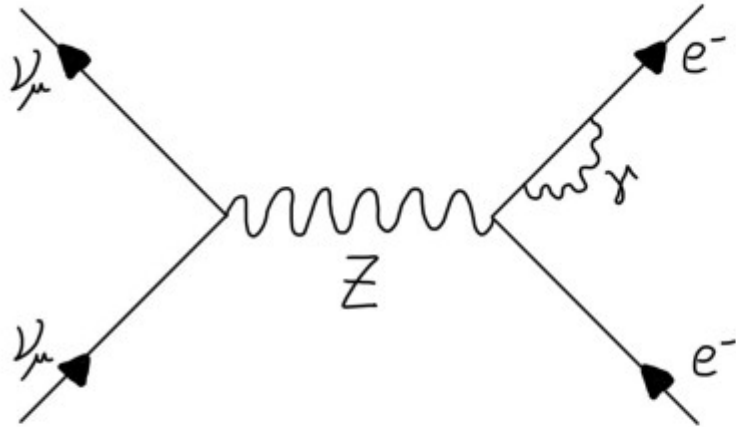
$$g_L = \frac{1}{2} - \sin^2 \theta_W \quad (2a)$$

and

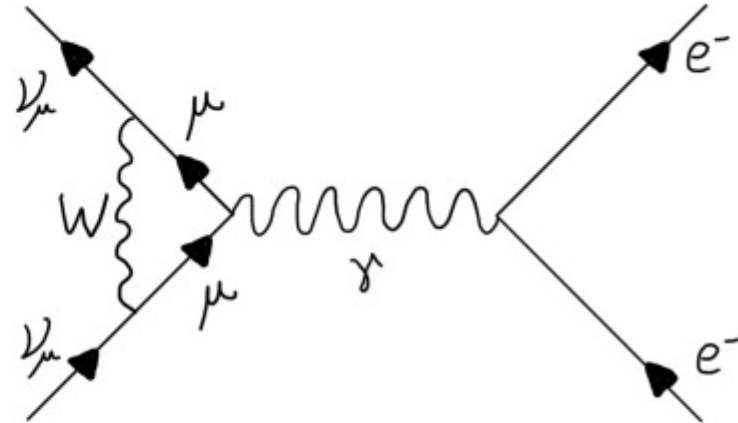
$$g_R = -\sin^2 \theta_W, \quad (2b)$$

where  $\theta_W$  is the weak mixing angle.

# Radiative corrections



(a) QED radiative correction.



(b) EW radiative correction.

Figure 1: Feynman diagrams representing high order radiative corrections from (a) QED,  $e\gamma e$  vertexes and (b) EW,  $\mu W \nu_\mu$  vertexes.

# Corrected cross section

The expression considering QED and EW radiative corrections for the  $\nu_\mu e^-$  differential cross section takes the form,

$$\frac{d\sigma'}{dT} = \frac{2m_e G_F^2}{\pi} \left\{ \underline{g_L'^2(T)} \left[ 1 + \frac{\alpha}{\pi} \underline{f_-(z)} \right] + \underline{g_R'^2(T)} \left( 1 - \frac{T}{E_\nu} \right)^2 \left[ 1 + \frac{\alpha}{\pi} \underline{f_+(z)} \right] - \underline{g_R'(T)g_L'(T)} m_e \frac{T}{E_\nu^2} \left[ 1 + \frac{\alpha}{\pi} \underline{f_{+-}(z)} \right] \right\}, \quad (3)$$

where the functions  $f_+(z)$ ,  $f_-(z)$ , and  $f_{+-}(z)$  account for the QED corrections that depend on  $z = T/E_\nu$ .  $\alpha$  is the fine-structure constant. The expressions for these functions [\[33\]](#) are given in Appendix [A](#). The values of  $f_+(z)$ ,  $f_-(z)$ , and  $f_{+-}(z)$  present important variations with the neutrino energy in the range under consideration. For the antineutrino cross section, the  $g'_{L,R}$  couplings must be interchanged like  $g'_L \leftrightarrow g'_R$ , while the three functions,  $f(z)$ , are preserved.

# Coupling constants

The coupling constants now include the EW corrections in the following way:

$$g'_L(T) = \underline{\rho_{\text{NC}}} \left[ \frac{1}{2} - \underline{\kappa_{\nu_l}(T)} \sin^2 \theta_W^{(m_Z)} \right] \quad (4a)$$

and

$$g'_R(T) = -\underline{\rho_{\text{NC}}} \underline{\kappa_{\nu_l}(T)} \sin^2 \theta_W^{(m_Z)}, \quad (4b)$$

where  $\rho_{\text{NC}}$  and  $\kappa_{\nu_l}(T)$  are defined in Eqs. (5) and (6) below.  $m_Z$  is the  $Z$  boson mass and  $\sin^2 \theta_W^{(m_Z)}$  is  $\sin^2 \theta_W$  calculated at the  $m_Z$  scale.

# First approach – monoenergetic beam

$$g'_L(T) = \rho_{\text{NC}} \left[ \frac{1}{2} - \kappa_{\nu_l}(T) \sin^2 \theta_W^{(mz)} \right] \longrightarrow \tilde{g}_L \approx \frac{1}{2} - \kappa_{\nu_\mu} x \quad \text{For a fixed } E_\nu,$$

$$g'_R(T) = -\rho_{\text{NC}} \kappa_{\nu_l}(T) \sin^2 \theta_W^{(mz)}, \quad \longrightarrow \quad \tilde{g}_R \approx -\kappa_{\nu_\mu} x, \quad \text{where,} \quad x = \sin^2 \theta_W$$

$$R_X := \frac{\frac{d\sigma'_X}{dT} - \frac{d\sigma}{dT}}{\frac{d\sigma}{dT}},$$

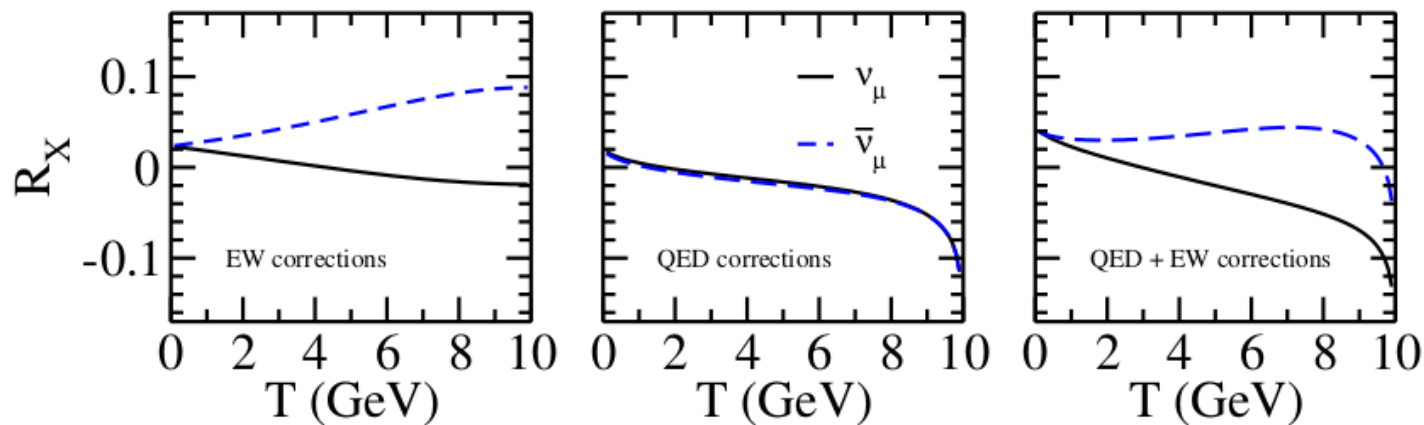


Figure 2: Comparison of the ratio of radiative corrections for neutrino and antineutrino beam modes, for a fixed neutrino energy of 10 GeV. a) Contribution of EW corrections, b) contribution of QED corrections, and c) total contributions.

# $\kappa$ dependence on $q^2$

Rho has the numerical value  $\rho_{\text{NC}} = 1.014032$ . (5)

$$\begin{aligned} \kappa_{\nu_l}(q^2) = 1 - \frac{\alpha}{2\pi\hat{s}^2} & \left[ \sum_i (C_{3i}Q_i - 4\hat{s}^2Q_i^2) J_i(q^2) - 2J_l(q^2) \right. \\ & \left. + \ln c \left( \frac{1}{2} - 7\hat{c}^2 \right) + \frac{\hat{c}^2}{3} + \frac{1}{2} + \frac{\hat{c}_\gamma}{\hat{c}^2} \right], \end{aligned} \quad (6)$$

where  $C_{3i}$  is twice the third component of weak isospin,  $Q_i$  represents the electric charge,  $\hat{c}_\gamma = \frac{19}{8} - \frac{17}{4}\hat{s}^2 + 3\hat{s}^4$ ,  $q^2 = -2m_e T$  is the squared four-momentum transfer, and

$$J_i(q^2) = \int_0^1 x(1-x) \ln \left( \frac{m_i^2 - q^2 x(1-x)}{m_Z^2} \right) dx, \quad (7)$$

where  $m_i$  is the mass of the  $i$ th fermion. The sum in Eq. (6) includes all the charged fermions, and we consider an additional factor of 3 for quarks (due to the color degree of freedom).

# $\kappa$ and its contributions

$$\kappa_\nu(q^2) = 1 - \frac{\alpha}{2\pi\hat{s}^2} \left[ \sum_i (C_{3i}Q_i - 4\hat{s}^2Q_i^2) J_i(q^2) + \ln c \left( \frac{1}{2} - 7\hat{c}^2 \right) + \frac{\hat{c}^2}{3} + \frac{\hat{c}_\gamma}{\hat{c}^2} \right].$$

In the energy region of interest for this work, this contribution takes the value  $\kappa_\nu(q^2) = 1.017$ .

The second contribution is flavor dependent,

$$-\frac{\alpha}{2\pi\hat{s}^2} \left[ -2J_l(q^2) + \frac{1}{2} \right],$$

and its numerical value in this region is  $-0.025$ .

# Neutrino Charge Radius

$$-2J_l(0) + \frac{1}{2} = \frac{1}{6} \left[ 3 - 2 \ln \left( \frac{m_l^2}{m_Z^2} \right) \right].$$

This quantity <sup>1</sup> is usually associated with the neutrino charge radius (NCR),

$$\langle r_{\nu_l}^2 \rangle = \frac{G_F}{4\sqrt{2}\pi^2} \left[ 3 - 2 \ln \left( \frac{m_l^2}{m_W^2} \right) \right],$$

for which the reported value for the  $\mu$  flavor is  $\langle r_{\nu_\mu}^2 \rangle = 2.4 \times 10^{-33} \text{ cm}^2$  [11].

---

<sup>1</sup>The right-hand side of Eq. (16) can be written in terms of  $m_W$  adding  $\frac{1}{3} \ln \left( \frac{m_W^2}{m_Z^2} \right)$  to it. In the shaded region of Fig. 3, we have  $\kappa_{\nu_\mu}^{(m_Z)} = 0.9921$  and  $\kappa_{\nu_\mu}^{(m_W)} = 0.9925$ , only a  $\sim 0.04\%$  difference.

# Neutrino Charge Radius

- The **straight-forward definition** of a neutrino charge radius has been proven to be **gauge-dependent**;
- The definition we use is an **attempt to define a physically observable** neutrino charge radius;
- A more general interpretation of the **experimental results** is that they are limits on certain **nonstandard contributions to neutrino scattering**.

# Prediction depending on NRC

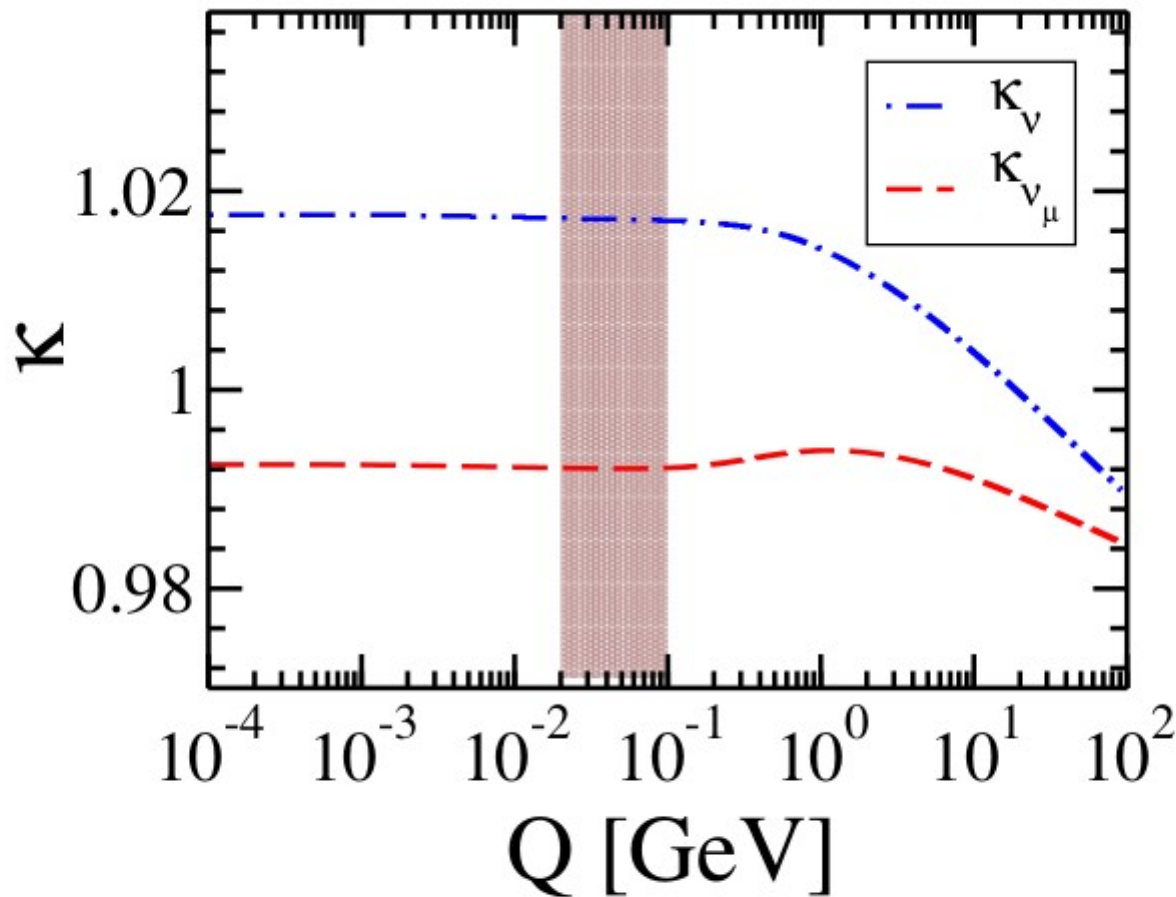
We can also separate the couplings  $g'_L(T)$  and  $g'_R(T)$  into two parts, one independent of the incoming neutrino flavor and the other in terms of the NCR as [11],

$$g'_{L,R}{}^{(\nu_\mu,e)}(T) \sim g'_{L,R}{}^{(\nu,e)}(T) + \left[ \frac{2}{3} m_W^2 \langle r_{\nu_\mu}^2 \rangle \right] \sin^2 \theta_W^{(mz)}, \quad (18)$$

where the numerical value of  $\left[ \frac{2}{3} m_W^2 \langle r_{\nu_\mu}^2 \rangle \right] \sin^2 \theta_W^{(mz)}$  is  $\approx 0.0058$ .

Table 1: Numerical value of  $\kappa$  (evaluated at  $q^2 = 0$ ) and of the couplings  $g'_L(T)$  and  $g'_R(T)$ , depending on the inclusion of the neutrino charge radius term.

NCR	$\kappa$	$g'_L$	$g'_R$
no	1.0176	0.2684	-0.2386
yes	0.9925	0.2743	-0.2327



$$Q \equiv \sqrt{-q^2}$$

$$q^2 = -2m_e T$$

Figure 3:  $\kappa_\nu$  and  $\kappa_{\nu_\mu}$  as functions of  $Q$ . The dot-dashed blue line represents  $\kappa_\nu$ , Eq. (14), and the dashed red line represents  $\kappa_{\nu_\mu}$ , Eq. (6). The shaded area represents the electron recoil energy ( $T$ ) where we investigate the effect of radiative corrections and the experimental sensitivity to the neutrino charge radius.

# Number of events

$$\sigma = \int_{T_{min}}^{T_{max}} f(T) dT, \quad (19)$$

where  $f(T)$  is the integral of the differential cross section,  $\frac{d\sigma}{dT}(T, E_\nu)$ , times the corresponding neutrino flux,  $\lambda(E_\nu)$ ,

$$f(T) = \int_{E_\nu^{min}(T)}^{E_\nu^{max}} \frac{d\sigma}{dT}(T, E_\nu) \lambda(E_\nu) dE_\nu, \quad (20)$$

where  $E_\nu^{min}(T)$  is the minimum neutrino energy considered and given by the detector's electron energy threshold.

Once we compute the cross section, Eq. (19), it is necessary to take into account the detector exposure to obtain the number of events,

$$N = \sigma \times \mathcal{C}, \quad (21)$$

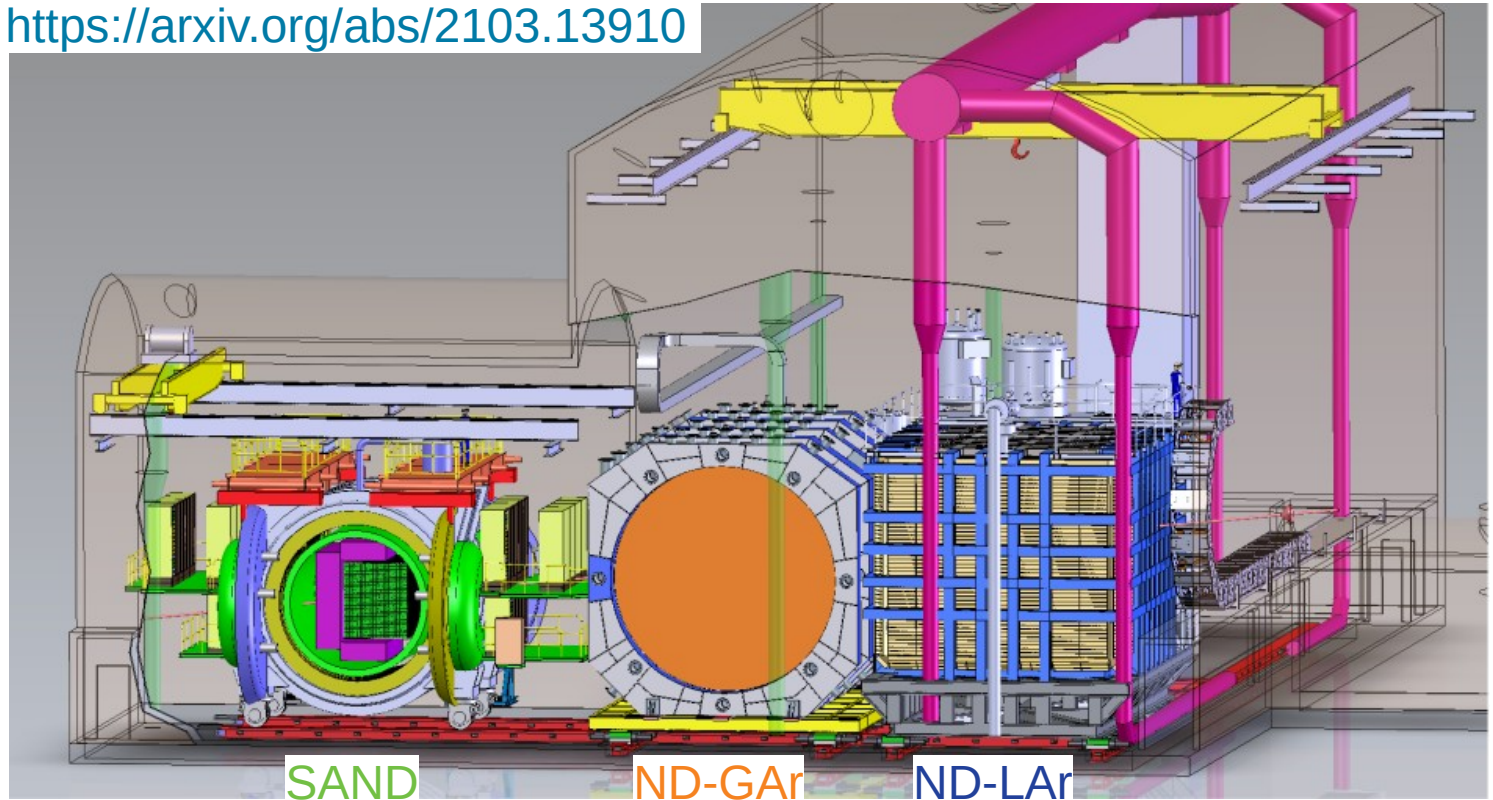
where  $\mathcal{C}$  is the exposure. It takes into account the number of target electrons in the detector, the number of protons on target per year of  $1.1 \times 10^{21}$  POT/year [45], and 3.5 years in the neutrino beam mode plus 3.5 years in the antineutrino beam mode.

# DUNE Near Detector – case study

Located 574 m from beam target

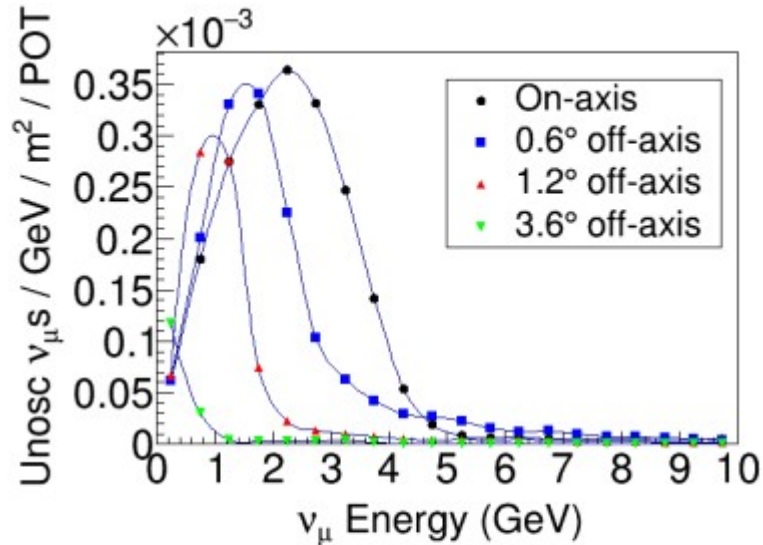
- Multiple complementary systems;
- Measure the neutrino flux;
- Monitor time variation of beam;
- Constrain cross-section models and systematic uncertainties.

<https://arxiv.org/abs/2103.13910>

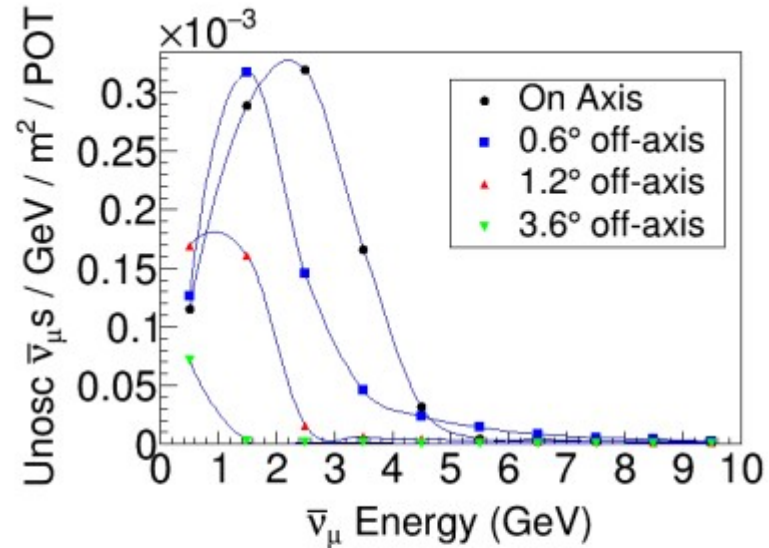


**PRISM can move off-axis up to 33 m (different beam fluxes, characterize beam, and constrain systematic uncertainties)**

# Fluxes for DUNE-PRISM



(a)  $\nu_\mu$  beam mode



(b)  $\bar{\nu}_\mu$  beam mode

Figure 4: Fluxes at several off axis locations [45]. Neutrino mode (a), on the left side, and antineutrino mode (b), on the right side. The symbols represent the simulated data, and the lines show their interpolation.

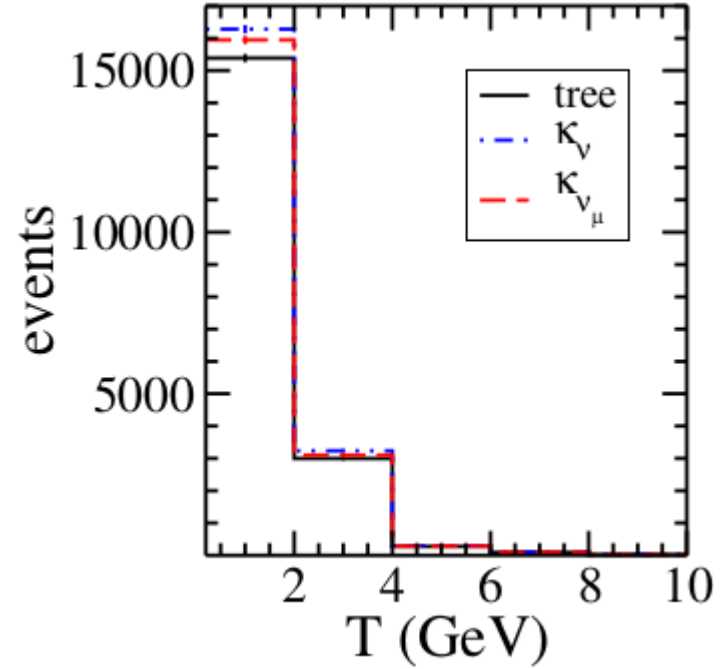
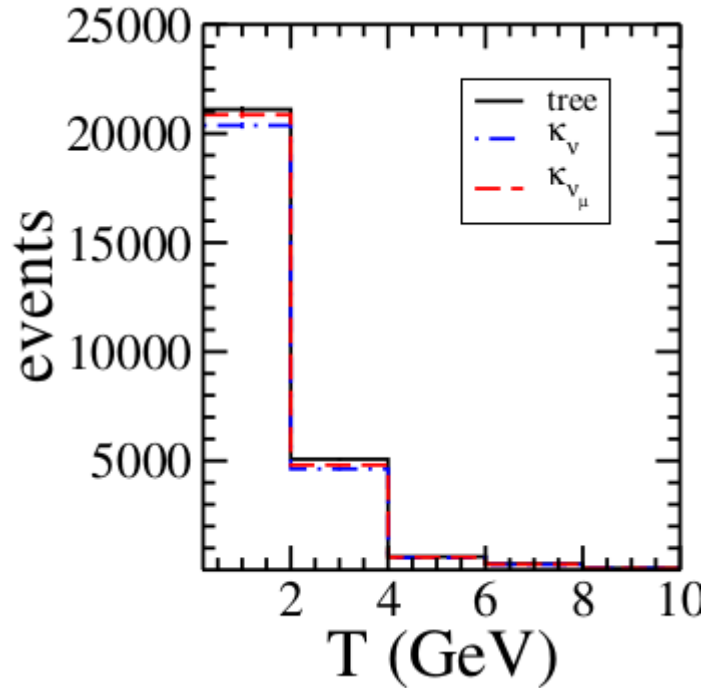
Table 2: The total number of events from  $\bar{\nu}_\mu e$  scattering for an energy range of 0.2 to 10 GeV, considering the tree level and radiative corrections with and without neutrino charge radius (NCR). The first column shows the DUNE-PRISM axis location.  $\sigma_{stat}$  is the statistical error and  $\Delta$  is the difference between the number of events calculated at tree level and with radiative corrections. See text for details.

	Number of $\bar{\nu}_\mu$ Events					
			Without NCR		With NCR	
Axis location	Tree level	$\sigma_{stat}$	EW+QED	$\Delta$	EW+QED	$\Delta$
0.0°	18775	137	19931	1156	19447	672
0.6°	11969	109	12715	746	12402	433
1.2°	3993	63	4251	258	4141	148
1.8°	1181	34	1260	79	1226	45
2.4°	645	25	689	44	670	25
3.0°	437	21	467	30	454	17
3.6°	315	18	336	21	327	12

Table 3: The total number of events from  $\nu_\mu e$  scattering for an energy range of 0.2 to 10 GeV, considering the tree level and radiative corrections with and without neutrino charge radius. The first column shows the DUNE-PRISM axis location.  $\sigma_{stat}$  is the statistical error and  $\Delta$  is the difference between the number of events calculated at tree level and with radiative corrections. See text for details.

Axis location	Number of $\nu_\mu$ Events					
	Tree level	$\sigma_{stat}$	Without NCR		With NCR	
			EW+QED	$\Delta$	EW+QED	$\Delta$
0.0°	27134	165	25859	-1275	26567	-567
0.6°	18099	135	17243	-856	17712	-387
1.2°	5884	77	5589	-295	5749	-135
1.8°	2600	51	2466	-134	2538	-62
2.4°	1397	37	1324	-73	1364	-33
3.0°	711	27	674	-37	694	-17
3.6°	440	21	418	-22	430	-10

# Number of $\nu$ (left) and $\bar{\nu}$ (right) on-axis events



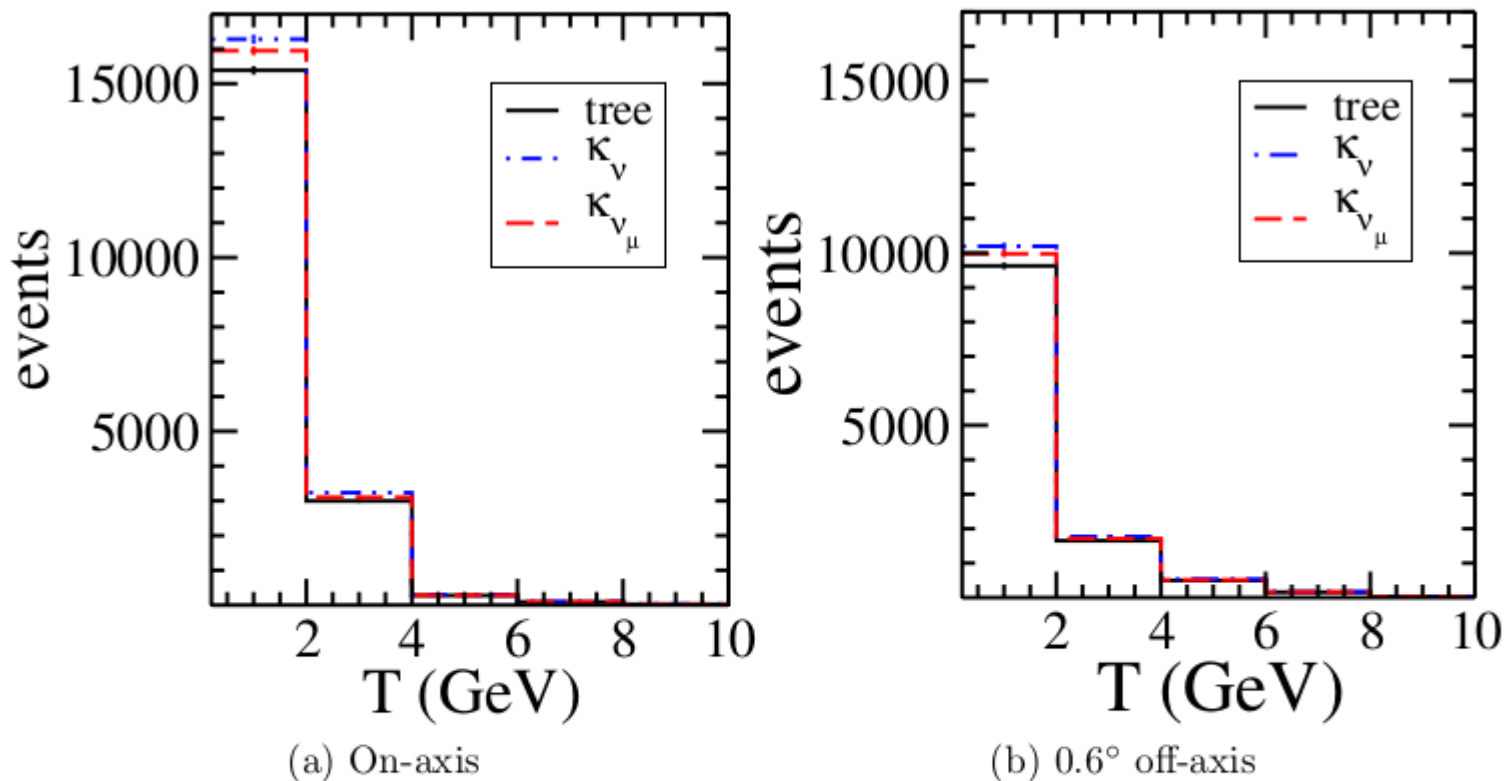


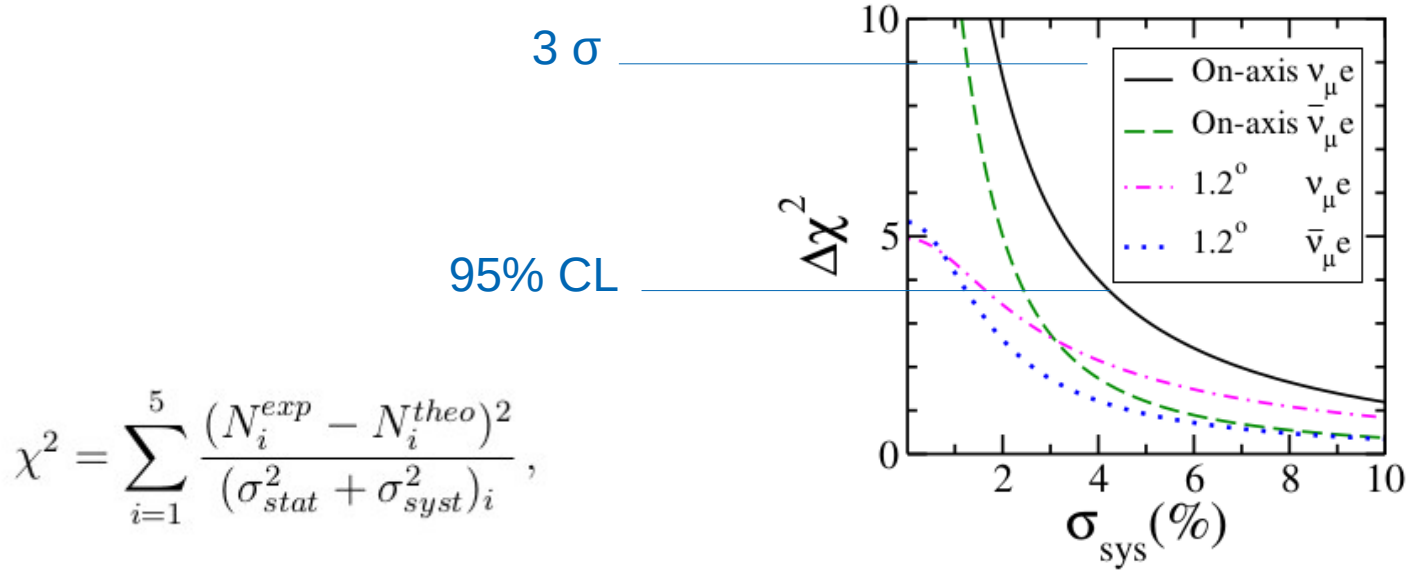
Figure 5: Comparison among the number of  $\bar{\nu}_\mu$  event expectations at tree-level (solid black line) and considering radiative corrections, with and without neutrino charge radius (dashed red and dot-dashed blue line, respectively). We show two DUNE-PRISM spectra: (a) On axis on the left and (b)  $0.6^\circ$  on the right side.

# Event number comparison

Table 4: The total number of events for  $\bar{\nu}_\mu$  and  $\nu_\mu$  beam modes, on axis, within the energy range from 0.7 to 10 GeV, considering the tree level and radiative corrections with and without neutrino charge radius.  $\sigma_{stat}$  is the statistical error and  $\Delta$  is the difference between the number of events calculated at tree level and with radiative corrections. See text for details.

	Number of Events					
			Without NCR		With NCR	
	Tree level	$\sigma_{stat}$	EW+QED	$\Delta$	EW+QED	$\Delta$
$\bar{\nu}_\mu$	12935	114	13850	915	13420	485
$\nu_\mu$	19947	141	18715	-1232	19318	-629

# Expected sensitivity to RC



$$\chi^2 = \sum_{i=1}^5 \frac{(N_i^{\text{exp}} - N_i^{\text{theo}})^2}{(\sigma_{\text{stat}}^2 + \sigma_{\text{syst}}^2)_i},$$

Figure 8: Expected sensitivity, in terms of  $\Delta\chi^2 = \chi^2 - \chi_{\text{min}}^2$ , to differentiate between the tree level and the radiative corrections case, depending on the systematic error. We show the results for two different locations of the detector (on axis and  $1.2^\circ$ ) and for neutrino (solid and dash-dotted) and antineutrino (dashed and dotted) electron scattering. For the neutrino electron case, we have chosen an energy threshold of 0.7 GeV to improve the sensitivity.

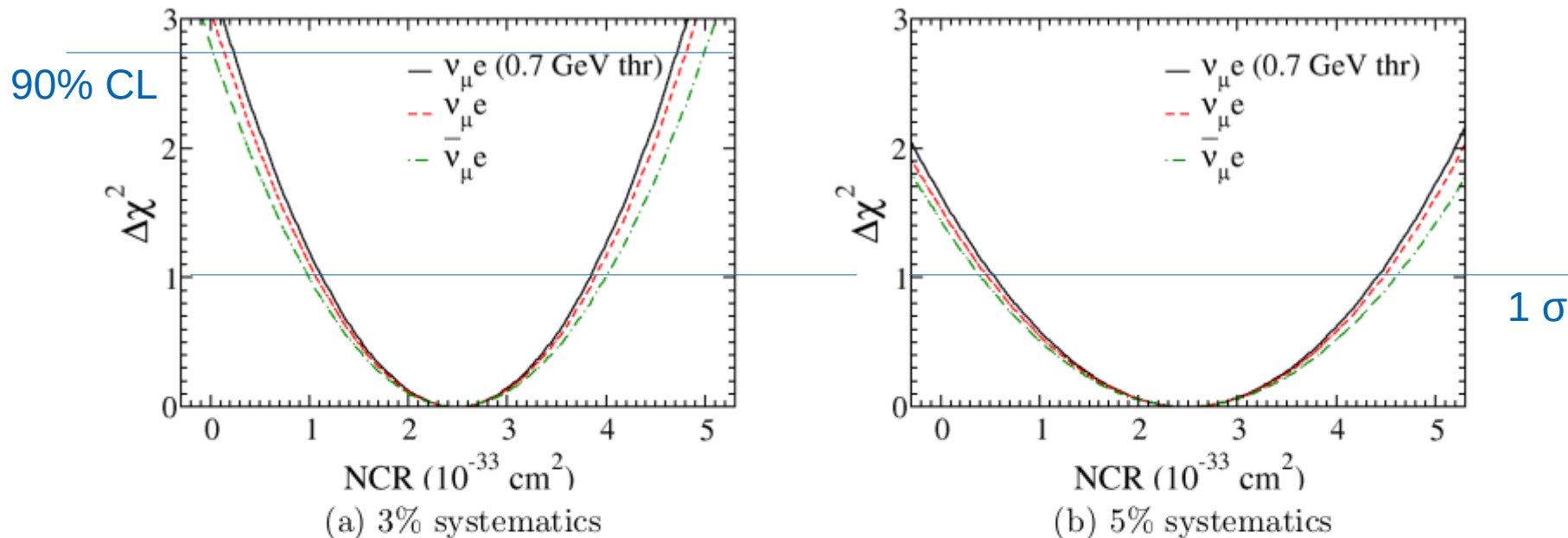


Figure 7: Expected sensitivity to the electroweak radiative corrections for a 3% systematic error (a) Left; and 5% systematic error (b) Right. We show  $\Delta\chi^2 = \chi^2 - \chi_{\min}^2$  as a function of the neutrino charge radius (NCR). Red dashed and green dot-dashed lines correspond to a 0.2 GeV threshold in the  $\nu$  and  $\bar{\nu}$  scattering, while the black line corresponds to the 0.7 GeV  $\nu$  scattering threshold. Neutrino data with 0.7 GeV threshold and 3% systematic error can reach a better than 90% confidence level sensitivity to the NCR within our assumptions. See text for details.

# PDG Limits on NCR

<u>VALUE (<math>10^{-32} \text{ cm}^2</math>)</u>	<u>CL%</u>	<u>DOCUMENT ID</u>	<u>TECN</u>	<u>COMMENT</u>
– <b>2.1 to 3.3</b>	90	<sup>1</sup> DENIZ	10 TEXO	Reactor $\bar{\nu}_e e$
● ● ● We do not use the following data for averages, fits, limits, etc. ● ● ●				
– 27.5 to 3	90	<sup>2</sup> CAEDDU	18	$\nu_\mu$ coherent scat. on CsI
– 0.53 to 0.68	90	<sup>3</sup> HIRSCH	03	$\nu_\mu e$ scat.
– 8.2 to 9.9	90	<sup>4</sup> HIRSCH	03	anomalous $e^+ e^- \rightarrow \nu \bar{\nu} \gamma$
– 2.97 to 4.14	90	<sup>5</sup> AUERBACH	01 LSND	$\nu_e e \rightarrow \nu_e e$
– 0.6 to 0.6	90	VILAIN	95B CHM2	$\nu_\mu e$ elastic scat.
0.9 $\pm$ 2.7		ALLEN	93 CNTR	LAMPF $\nu e \rightarrow \nu e$
< 2.3	95	MOURAO	92 ASTR	HOME/KAM2 $\nu$ rates
< 7.3	90	<sup>6</sup> VIDYAKIN	92 CNTR	Reactor $\bar{\nu} e \rightarrow \bar{\nu} e$
1.1 $\pm$ 2.3		ALLEN	91 CNTR	Repl. by ALLEN 93
– 1.1 $\pm$ 1.0		<sup>7</sup> AHRENS	90 CNTR	$\nu_\mu e$ elastic scat.
– 0.3 $\pm$ 1.5		<sup>7</sup> DORENBOS...	89 CHRM	$\nu_\mu e$ elastic scat.
		<sup>8</sup> GRIFOLS	89B ASTR	SN 1987A

P.A. Zyla et al. (Particle Data Group), Prog. Theor. Exp. Phys. 2020 , 083C01 (2020) and 2021 update

# Conclusions

- DUNE-like ND is capable of measuring electroweak theory radiative correction effects;
- In order to improve sensitivity we need higher flux at low energies;
- A 90% CL NCR indication is possible in this case study, as long as the systematic uncertainties are below  $\sim 3\%$ .

Thank you!

# ND-LAr requirements/capabilities

- Comparable to FD;
- Measure the neutrino flux;
- Reconstruct the neutrino energy;
- Measure the energy spectrum;
- Validate modeling of  $\nu_e$  background...

# ND-GAr requirements/capabilities

- Track, identify the sign, and momentum-analyze muons exiting ND-LAr;
- Measure the energy spectrum of  $\nu_\mu$  and  $\bar{\nu}_\mu$  charged current interactions that occur in ND-LAr;
- Clarify the relationship between true and reconstructed energy by studying neutrino interactions on argon;
- Sensitive to low energy charged tracks, photons, and neutrons;
- Greatly extends the particle ID performance, particularly for proton-pion separation...

# System for on-Axis Neutrino Detection - SAND

- Continuous on-axis beam monitoring system;
- Have muon or neutrino energy resolution in  $\nu_\mu$  events to detect spectral variations;
- provide an independent measurement of the interaction rate and energy spectra of the  $\nu_\mu$ ,  $\bar{\nu}_\mu$ , and  $\nu_e$ ,  $\bar{\nu}_e$  beam components;
- complementary measurements of both the normalization and energy dependence of the flux...

# Neutrino Charge Form Factor and NCR

$$f_Q(q^2) = f_Q(0) + q^2 \left. \frac{df_Q(q^2)}{dq^2} \right|_{q^2=0} + \dots$$

$$f_Q(q^2) = \int \rho(r) e^{-i\vec{q}\cdot\vec{x}} d^3x = \int \rho(r) \frac{\sin(|\vec{q}|r)}{|\vec{q}|r} d^3x.$$

$$\lim_{q^2 \rightarrow 0} \frac{df_Q(q^2)}{dq^2} = \int \rho(r) \frac{r^2}{6} d^3x = \frac{\langle r^2 \rangle}{6}$$